Acta Crystallographica Section D
Biological Crystallography
ISSN 0907-4449

Determination of a protein structure by iodination: the structure of iodinated acetylxylan esterase

Debashis Ghosh,[a,b]* Mary Erman,[a] Mark Sawicki,[b] Puloma Lala,[b] Daniel R. Weeks,[a] Naiyin Li,[a] Walter Pangborn,[a] Daniel J. Thiel,[c] Hans Jörnvall,[d] Rodrigo Gutierrez[e]† and Jaime Eyzaguirre[e]

[a]Hauptman-Woodward Medical Research Institute, 73 High Street, Buffalo, New York 14203, USA, [b]Roswell Park Cancer Institute, Buffalo, New York, USA, [c]Cornell High Energy Synchrotron Source, Ithaca, New York, USA, [d]Karolinska Institutet, Stockholm, Sweden, and [e]Pontificia Universidad Catolica de Chile, Santiago, Chile

† Present address: Michigan State University, East Lansing, Michigan, USA.

Correspondence e-mail: ghosh@hwi.buffalo.edu

Received 9 October 1998
Accepted 5 January 1999

PDB References: acetylxylan esterase, 1bs9; iodinated acetylxylan esterase, 2axe.

Enzymatic and non-enzymatic iodination of the amino acid tyrosine is a well known phenomenon. The iodination technique has been widely used for labeling proteins. Using high-resolution X-ray crystallographic techniques, the chemical and three-dimensional structures of iodotyrosines formed by non-enzymatic incorporation of I atoms into tyrosine residues of a crystalline protein are described. Acetylxylan esterase (AXE II; 207 amino-acid residues) from *Penicillium purpurogenum* has substrate specificities towards acetate esters of D-xylopyranose residues in xylan and belongs to a new class of α/β hydrolases. The crystals of the enzyme are highly ordered, tightly packed and diffract to better than sub-ångström resolution at 85 K. The iodination technique has been utilized to prepare an isomorphous derivative of the AXE II crystal. The structure of the enzyme determined at 1.10 Å resolution exclusively by normal and anomalous scattering from I atoms, along with the structure of the iodinated complex at 1.80 Å resolution, demonstrate the formation of covalent bonds between I atoms and C atoms at *ortho* positions to the hydroxyl groups of two tyrosyl moieties, yielding iodotyrosines.

1. Introduction

I atoms can be incorporated enzymatically or non-enzymatically into tyrosine residues of proteins, forming iodotyrosines (Morrison & Schonbaum, 1976; Taurog *et al.*, 1996; Huwiler *et al.*, 1985). Iodination is used for labeling proteins in a wide variety of experiments, such as protein-metabolism studies and radioimmunoassay (Morrison & Schonbaum, 1976). Incorporation of iodine into the amino acid tyrosine is carried out enzymatically in thyroid follicles by thyroid peroxidase, resulting in the formation of monoiodo- and diiodotyrosines. Two iodotyrosines are then coupled, leading to the biosynthesis of two important thyroid hormones, triiodo- and tetraiodothyronine (Morrison & Schonbaum, 1976; Taurog *et al.*, 1996). In the 1960s, attempts were made to use iodination of protein crystals both for labeling tyrosine and histidine residues to serve as guides for building protein models into electron-density maps and for phase determination and solution of protein structures (Kenkare & Richards, 1966; Kretsinger, 1968; Cohen *et al.*, 1969; Sigler, 1970). Sigler presented the crystallographic evidence to demonstrate that in α-chymotrypsin iodination resulted in the formation of a diiodotyrosine (Sigler, 1970). However, although efforts to utilize iodination in crystals met with occasional successes, *ab initio* determination of crystallographic phases by iodination alone at a resolution suitable for building protein models was

not achieved. Furthermore, to our knowledge, detailed structural characterization of iodinated tyrosyl products in proteins has not previously been carried out by crystallography or any other method.

Acetylxylan esterase (AXE II; 207 amino-acid residues, E.C. 3.1.1.6) from *Penicillium purpurogenum* has substrate specificities towards acetate esters of D-xylopyranose residues in xylan and belongs to a new class of α/β hydrolases (Egana *et al.*, 1996; Gutierrez *et al.*, 1998). The crystals of the enzyme are highly ordered, tightly packed and diffract to better than subångström resolution at 85 K (Pangborn *et al.*, 1996). In the absence of any AXE structure which could be used as a search model, an *ab initio* solution of the structure had to be pursued. However, conventional techniques for the preparation of heavy-atom derivatives (using Hg, Pt, Au *etc*. salts) for the *ab initio* phase determination and attempts towards direct phase determination using techniques applicable to macromolecular data at atomic resolution (Weeks *et al.*, 1994) were unsuccessful. Iodination proved to be the technique of choice for producing an excellent isomorphous derivative.

2. Experimental procedures

We treated the crystals of AXE II with a solution of molecular iodine in potassium iodide and were able to produce a derivative crystal highly isomorphous to the native crystals to at least 2.00 Å resolution. We collected a complete 1.80 Å diffraction data set from one iodinated derivative crystal. An electron-density map computed at 2.00 Å resolution (Fig. 1) derived exclusively from single isomorphous and anomalous scattering (SIRAS) data of the iodine derivative of the AXE II crystal led to complete tracing of the polypeptide chain and subsequent refinement of the three-dimensional structure at 1.10 Å resolution.

2.1. Crystallization, iodination and data collection

Crystallization and data-collection experiments at the Cornell High Energy Synchrotron Source (CHESS) have previously been described (Pangborn *et al.*, 1996). The enzyme was crystallized from ammonium sulfate solution in 50 m*M* citrate buffer at pH 5.3. The data set at ambient temperature was collected at the F-2 station of CHESS using a 2K CCD detector and processed with *DENZO* (Otwinowski & Minor, 1995). A total of 149250 observations were measured from one crystal, yielding 44040 unique data with an $R_{\rm merge}$ on intensities of 0.054. The data was 83.5% complete to 1.39 Å and 69.3% complete to 1.10 Å resolution. The completion rate was 44.9% in the 1.14–1.10 Å resolution shell, and the average intensity-to-standard-deviation ratio for that shell was 4.0. The space group was $P2_12_12_1$ and the unit-cell parameters were a = 34.95, b = 61.05, c = 72.61 Å, with one molecule in the asymmetric unit.

The iodination experiment was carried out by soaking the crystals in a freshly prepared solution of I_2 in KI. The optimal soaking condition was established by trial and error; the range of final I_2 concentrations in the soaking solution was 0.05–5.0 m*M*. The soaking time varied between several hours and 60 d. Depending on the soaking conditions, the colorless crystals often turned dark red. Interestingly, AXE II crystals which could not be destroyed by hours of exposure to synchrotron X-rays at ambient temperature or weeks of soaking in various heavy-atom compounds, lost all their diffraction when soaked for a few days in I_2 solutions of concentrations of 1 m*M* or greater, although no physical damage was visible. The crystal used for data collection was soaked in a 0.1 m*M* I_2 solution for 60 d and had a yellowish tinge. The diffraction data on the iodinated crystal was collected at the in-house R-AXIS IIc image-plate detector at ambient temperature, with Cu $K\alpha$ X-ray from a rotating-anode generator. There were 15046 unique reflections for a total of 99865 observations with an $R_{\rm merge}$ of 0.11. The data was 99.8% complete to 1.80 Å.

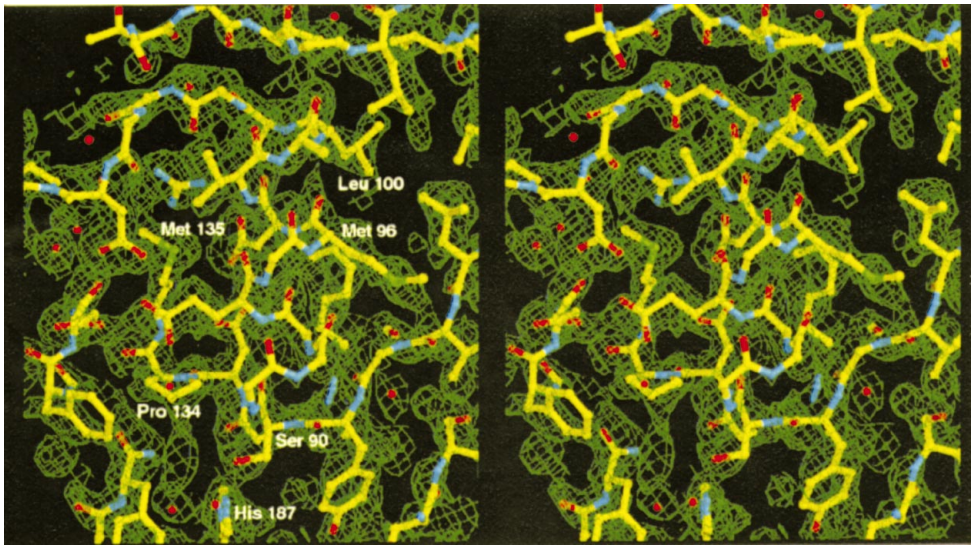

Figure 1
A typical SIRAS electron-density map of AXE II showing an α-helix, β-strands and turn and loop regions. The map, based solely upon the isomorphous and anomalous scattering contributions from I atoms, has a limiting resolution of 2.00 Å and is contoured at 1σ. The model shown is the refined native molecule. Some of the residues, including the catalytic Ser90 and His187, are labeled. The illustration was produced using *Raster3D* (Merritt & Bacon, 1997).

2.2. Structure solution and refinement

The scaling R factor between the native and iodine-derivative structure amplitudes was 0.19. The difference amplitude fell away monotonically between 99.0 and 2.00 Å, thus exhibiting an excellent isomorphism between the native and the derivative crystals.

Table 1
Refinement statistics.

	1.80 Å resolution	1.10 Å resolution
Protein atoms in the model	1442	1442
I atoms	4	0
Number of protein residues with multiple conformations	2	4
Solvent sulfates	1	1
Solvent waters	91	167
Resolution range (Å)	99.0–1.80	99.0–1.10
Unique data used ($F > 0$)	15003	44020
Overall completeness (%)	99.8	69.3
wR^2	0.384	0.295
Crystallographic R		
All data	0.173	0.124
$F > 4\sigma F$	0.149	0.112
R_{free}		
All data	0.237	0.173
$F > 4\sigma F$	0.214	0.161
Goodness of fit	3.35	2.70
Restrained goodness of fit	2.69	2.26
R.m.s. deviations		
Bond distances (Å)	0.005	0.011
Bond angles (°)	1.783	2.094
Dihedral angles (°)	26.801	25.978
Planarity (°)	1.209	1.465
Ramachandran plot statistics		
Residues of 168 non-glycine and non-proline in most favored regions (%)	90.5	91.1

The iodine-binding sites were determined from difference Patterson synthesis using *HASSP* (Terwilliger & Eisenberg, 1983) and refined by the origin-removed difference Patterson technique using *HEAVY* (Terwilliger & Eisenberg, 1983). The final phase calculations and combination of isomorphous and anomalous phases were carried out using *PHASES* (Furey & Swaminathan, 1990). The centric R factor was 0.49 to 2.00 Å and the phasing powers for the isomorphous and anomalous components were 2.40 and 3.24, respectively. The figure of merit was 0.64 to 2.00 Å. The correctness of the choice of 'hand' of iodine positions was confirmed by the appearance of right-handed α-helices in the electron-density map.

A complete atomic model of the protein was built into this SIRAS map. The software *CHAIN* (Sack, 1988) and *XTALVIEW* (McRee, 1997) and a Silicon Graphics Indigo 2 workstation were used for the purpose. This starting model was then refined against both native and iodinated-complex data, initially by *X-PLOR* (Brünger, 1997) and then by *SHELX*97 (Sheldrick, 1997). The resolutions were gradually extended to the maximum limits of both data sets. Solvent molecules were then included in the models. The refinement of the native model was carried out using anisotropic temperature factors for the protein atoms. For the iodinated complex, the C—I bond distances were not restrained. A summary of refinement results is provided in Table 1. Details of the refinement procedure will be published elsewhere.

3. Results

A SIRAS electron-density map calculated at 2.00 Å resolution exclusively from the isomorphous and anomalous scattering differences from I atoms is shown in Fig. 1. A complete atomic model of the enzyme was built into this density map. A summary of the refinement results is presented in Table 1. Results from the refinement with the 0.90 Å cryogenic data set (Pangborn *et al.*, 1996) and full description of the structure will be published elsewhere.

The crystal structure of AXE II and the catalytic triad Ser90–His187–Asp175 are shown in Fig. 2. The fold is similar to that of cutinase (Longhi *et al.*, 1997). The tertiary structure consists of a doubly wound α/β sandwich, having a central parallel β-sheet flanked by two parallel α-helices on each side. All ten Cys residues are involved in the formation of five intra-chain disulfide bridges. The catalytic cleft is located at the C-terminal end of the β-sheet near the center, bordered by the helical loop 183–193 from one side and the loop 105–113 containing an antiparallel pair of strands from the other. These two loops may play a critical role in substrate specificity and binding. The geometry and relative orientations of the side chains of the catalytic triad are similar to those previously observed in other members of the α/β hydrolase family, such as cholesterol esterase (Ghosh *et al.*, 1995).

Geometrical and thermal parameters of two tyrosyl moieties before and after iodination are given in Table 2. Tyr177, located at the catalytic cleft near the triad and the most exposed of all the tyrosine residues, is fully iodinated at the two positions *ortho* to the hydroxyl group. Shown in Fig. 3(*b*) are superimposed refined native and iodine-deriva-

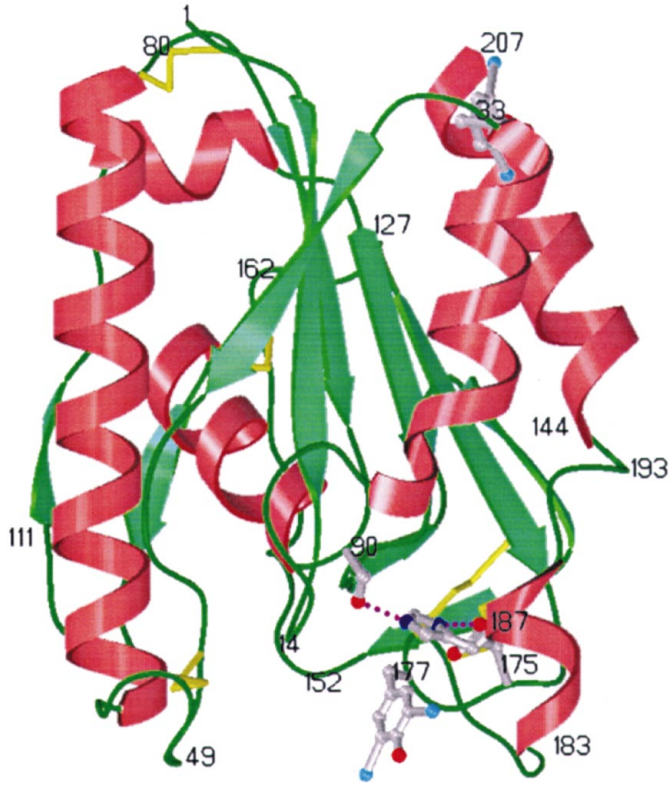

Figure 2
A ribbon diagram (*SETOR*; Evans, 1993) of the iodinated complex of AXE II showing the overall fold, the catalytic triad Ser90–His187–Asp175 and the iodotyrosine residues Tyr33 and Tyr177.

Table 2
Geometrical and thermal parameters for tyrosyl moieties before and after iodination reaction.

1.10 Å resolution.

	Tyr33	Tyr177
Centroid (x, y, z) (Å)	11.17, 15.94, 30.40	8.10, 8.35, −0.30
χ_1 (°)	−64.64	−51.69
χ_2 (°)	−81.09	−64.64
B_{ave} (Å^2)	14.96	28.88

1.80 Å resolution.

	Tyr33	Tyr177
Centroid (x, y, z) (Å)	11.15, 16.16, 30.27	8.19, 7.83, −0.44
χ_1 (°)	−61.81	−53.96
χ_2 (°)	−87.81	−59.18
B_{ave} (Å^2)	15.63	14.22

Deviation from planarity (1.80 Å resolution) (Å)

Tyr33			Tyr177		
I1	I2	R.m.s.d (all ten atoms)	I1	I2	R.m.s.d (all ten atoms)
−0.04	−0.26	0.14	−0.08	−0.13	0.06

Iodine parameters (1.80 Å resolution)

	Tyr33		Tyr177	
	I1	I2	I1	I2
SIRAS				
x (Å)	9.23	—	9.65	8.33
y (Å)	16.15	—	11.01	6.05
z (Å)	27.44	—	−0.31	−3.43
Occupancy	0.76	—	0.80	1.00
B (Å^2)	15.00	—	15.00	15.00
Refined				
x (Å)	9.29	9.57	9.56	8.30
y (Å)	16.27	15.05	11.04	6.15
z (Å)	27.40	33.49	−0.34	−3.43
Occupancy	1.00	0.25	1.00	1.00
B (Å^2)	29.94	50.85	29.24	21.71
C—I distance (Å)	2.09	2.43	2.10	2.11

tive structures of AXE II in the vicinity of Tyr177. The electron densities for 1.80 Å (without the iodine-bias) and 1.10 Å structures calculated from the respective refined models are also shown. A similar illustration for Tyr33 is shown in Fig. 3(*a*). The Tyr33 side chain is located at the other end of the molecule, away from the catalytic site, at the C-terminus of the α-helix 22–33. Interestingly, only three of these four I-atom positions could be located from the difference Patterson map with the native and iodine-derivative data (Table 2) prior to the complete tracing of the polypeptide chain. While these three iodine positions are fully occupied, the occupancy of the fourth iodine I2, linked to C$^{\varepsilon 2}$ of Tyr33, is only about 25% (Table 2). In 75% of molecules of the crystal, therefore, Tyr33 is a monoiodotyrosine. While the first three C—I distances range between 2.09 and 2.11 Å, similar to the average C—I distance of 2.095 Å in thyronine structures (Cody, 1974), the C$^{\varepsilon 2}$—I2 distance for Tyr33 is 2.43 Å (Table 2). The I atoms of Tyr177 deviate 0.08 and 0.13 Å, respectively, from the least-squares plane of the phenyl ring (Table 2). While the deviation of I1 from the Tyr33 phenyl ring is 0.04 Å, that of the 25% occupied I2 is 0.26 Å. Interestingly, the r.m.s. deviation from planarity for all atoms of the Tyr33 planar ring is higher than that of Tyr177.

The overall root-mean-square deviation between the C$^{\alpha}$ atoms of the native and iodinated-complex structures is

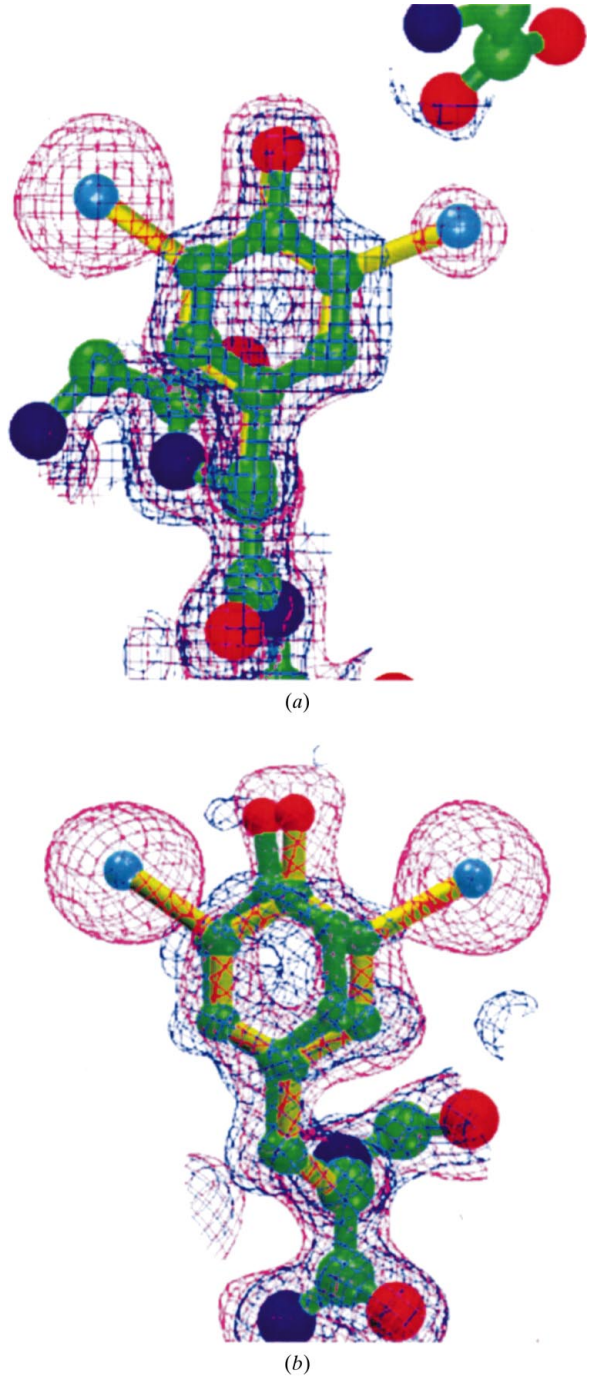

Figure 3
$2F_o - F_c$ electron-density maps for the native (blue; 1.10 Å resolution, contoured at 1.2σ) and iodinated complex (magenta; 1.80 Å resolution, contoured at 1.2σ) with their corresponding refined models (green, native; yellow, iodinated derivative) for (*a*) Tyr33 and (*b*) Tyr177. I atoms were not included in the phase calculation.

0.12 Å, reflecting a high degree of isomorphism. This isomorphism is represented in the proximity of the iodination sites as well, especially for the Tyr33 side chain. Iodination of this tyrosine moiety results in only a small translation of the centroid of the phenyl ring (0.21 Å) and change in the side-chain torsion angles (<7°) (Table 2). These values for Tyr177 are 0.54 Å and 6°, respectively, reflecting a larger movement of the side chain upon iodination (Fig. 3*b*). The average *B* factors of Tyr33 before and after iodination are also quite similar, being about 15 Å^2. The electron density of the highly exposed Tyr177 side chain is relatively weak in the native structure, consistent with its higher average *B* factor of 29 Å^2. However, the iodinated Tyr177 side chain has a well defined electron density and a lower average *B* value of 14 Å^2.

4. Discussion

The iodination reaction possibly involves a normal aromatic electrophilic substitution by iodonium ion obtained by oxidation of iodine. As depicted in Fig. 4, the iodination of tyrosine in all likelihood follows a mechanism similar to the halogenation of phenol in acidic conditions, as described in textbooks (Morrison & Boyd, 1973; Streitwieser & Heathcock, 1985). The presence of the electron-donating hydroxyl group makes the *ortho* position susceptible to iodination.

There are 11 tyrosine residues in AXE II. Accessibility calculations show that except for Tyr177, Tyr33 and, to some extent, Tyr19, all of these side chains are essentially buried within the protein molecule. The degree of iodination, therefore, appears to be a function of accessibility of the tyrosine side chain and exposure of the *ortho* C atoms to iodonium ions. The I atom linked to C$^{\varepsilon 2}$ of Tyr33 is only 25% occupied, in contrast to full occupancies of other three iodination sites. The C$^{\varepsilon 2}$ of Tyr33 is at a van der Waals contact distance of 3.9 Å from an oxygen of the C-terminal carboxyl group (Fig. 3*a*), possibly causing steric hindrance towards iodination of this C atom. The electron density for the terminal carboxyl group is weak in both structures and may be dynamically disordered, leading to partial iodination of C$^{\varepsilon 2}$. Furthermore, the C$^{\varepsilon 2}$—I2 distance for Tyr33 of 2.43 Å is suggestive of an intermediate

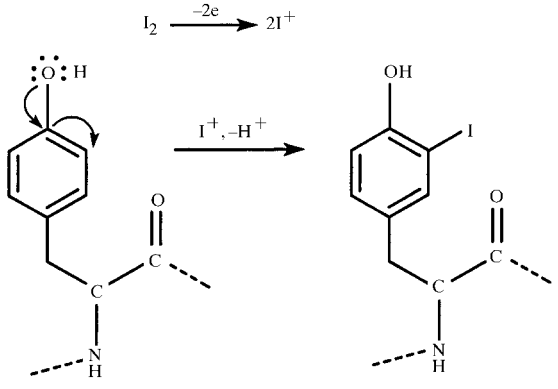

Figure 4
The mechanism of the iodination reaction could involve a normal aromatic electrophilic substitution by iodonium ion.

state towards the formation of a C—I covalent bond. The r.m.s. deviation from planarity for all atoms of the Tyr33 planar ring is higher than that of Tyr177, perhaps indicating partial localization of electrons and partial loss of planarity of the phenyl ring in transition. In addition, weakness and smearing of electron densities for C$^{\delta}$ and C$^{\varepsilon}$ atoms of Tyr177 in the native structure as well as their anisotropic thermal parameters suggest a rotational motion of the side chain about the C$^{\beta}$—C$^{\gamma}$ bond. Iodination appears to stabilize this motion and be responsible for lowering the average *B* factor of the side chain from 29 to 14 Å^2.

Proximity of any side chain does not appear to play a critical role in the iodination reaction, as the two tyrosyl moieties which are iodinated have different environments. The fully occupied I1 of Tyr33 sits in a hydrophobic pocket having van der Waals contacts (3.5–4.6 Å) with Val29 C$^{\gamma 1}$, Ala32 C$^{\beta}$, Leu199 C$^{\delta 1}$, Val202 C$^{\gamma 1}$, Lys203 C$^{\gamma}$ and Leu206 C$^{\delta 1}$ atoms. In the native structure, the Lys203 side chain (torsion angle χ_1) is in the *trans* conformation which changes to *cis* in the iodinated complex in order to accommodate the I atom. Iodines bonded to Tyr177, in comparison, are much more exposed; the atoms within contact distances of I1 are C atoms of the imidazole ring of His187 (4.0–4.1 Å). Protein atoms in contact with I2 (3.4–4.2 Å) are all from the Ser119–Asn123 segment of a symmetry-related molecule and hence contribute to packing interactions, including a contact with the Ser119 main-chain carbonyl O atom at a distance of 3.4 Å.

The use of anomalous scattering from atomic scatterers incorporated within crystalline protein molecules has become a popular technique for solving the phase problem in protein crystallography. The frequently used multiple-wavelength anomalous dispersion or MAD phasing method (Yang *et al.*, 1990), which utilizes the anomalous scattering from the Se atom incorporated into the protein molecule as a seleno-methionine by recombinant DNA technology, is one such example. Iodination of proteins in crystals could prove to be a very effective way to prepare a covalently linked heavy-atom derivative with a high degree of isomorphism, while at the same time providing an anomalous scatterer within the protein molecule. Our iodination technique is a simple trial-and-error approach to optimization of the soaking conditions by which a limited number of exposed tyrosines could be titrated with iodine. Admittedly, preparation of useful iodine derivatives of protein crystals could be quite tricky and this simple technique may not necessarily produce the desired iodination in all cases. Nevertheless, the results presented here demonstrate that derivative crystals highly isomorphous to native protein crystals can be prepared by this method and that iodination alone is sufficient to solve the phase problem. The method may prove useful in cases where tight packing and low solvent content of the crystal prevent traditional heavy-atom ions with large ionic radii from entering the access channels and where a suitable expression system for producing the recombinant protein is not available. The iodinated derivatives offer one additional advantage. In order to optimize the anomalous signal from selenium, the incident X-ray beam energy has to be tuned to the *K* absorption edge of the atom [0.979 Å; the

change in the real component of the atomic scattering factor ($\Delta f'$) is ~ -6.7 e and the change in the imaginary component of the atomic scattering factor ($\Delta f''$) is ~ 4.5 e; Yang *et al.*, 1990; *International Tables for X-ray Crystallography*, 1974, Vol. III, pp. 59–65] and the beam should be of high brilliance, which necessitate that the diffraction experiment be performed at a synchrotron X-ray source. The *K* and *L* absorption edges for iodine are 0.373 and 2.719 Å, respectively (*International Tables for X-ray Crystallography*, 1974, Vol. IV, p. 150). However, at the Cu $K\alpha$ edge, the most commonly used laboratory X-ray energy, the $\Delta f'$ and $\Delta f''$ values for iodine are ~ -0.6 e and ~ 6.8 e, respectively (*International Tables for X-ray Crystallography*, 1974, Vol. III, pp. 59–65). Our results show that these values are large enough to yield a significant anomalous signal and resolve the phase ambiguity. Therefore, the iodination technique for the preparation of heavy-atom derivatives of proteins could be a powerful method for solving the protein phase problem.

The authors wish to thank Professor George M. Sheldrick of Göttingen University for providing us with a copy of the *SHELX*97 software. JE thanks FONDECYT (Project IR 7960006) for financial support.

References

Brünger, A. T. (1997). *X-PLOR Manual* 3.8. Yale University, New Haven, Connecticut, USA.
Cody, V. (1974). *J. Am. Chem. Soc.* **96**, 6720–6725.
Cohen, G. H., Silverton, E. W., Matthews, B. W., Braxton, H. & Davies, D. R. (1969). *J. Mol. Biol.* **44**, 129–141.
Egana, L., Gutierrez, R., Caputo, V., Peirano, A., Steiner, J. & Eyzaguirre, J. (1996). *Biotechnol. Appl. Biochem.* **24**, 33–39.
Evans, S. V. (1993). *J. Mol. Graph.* **11**, 134–138.
Furey, W. & Swaminathan, S. (1990). Annu. Meet. Am. Crystallogr. Assoc., p. 73, Abstract PA33.
Ghosh, D., Wawrzak, Z., Pletnev, V. Z., Li, N., Kaiser, R., Pangborn, W., Jörnvall, H., Erman, M. & Duax, W. L. (1995). *Structure*, **3**, 279–288.
Gutierrez, R., Cederlund, E., Hjelmqvist, L., Peirano, A., Herrera, F., Ghosh, D., Duax, W., Jörnvall, H. & Eyzaguirre, J. (1998). *FEBS Lett.* **423**, 35–38.
Huwiler, M., Bürgi, U. & Kohler, H. (1985). *Eur. J. Biochem.* **147**, 469–476.
Kenkare, U. W. & Richards, F. M. (1966). *J. Biol. Chem.* **241**, 3197–3206.
Kretsinger, R. (1968). *J. Mol. Biol.* **31**, 315–318.
Longhi, S., Czjzek, M., Lamzin, V., Nicolas, A. & Cambillau, C. (1997). *J. Mol. Biol.* **268**, 779–799.
McRee, D. (1997). *XTALVIEW*. The Scripps Research Institute, San Diego, California, USA.
Merritt, E. & Bacon, D. J. (1997). *Methods Enzymol.* **277**, 505–524.
Morrison, M. & Schonbaum, G. R. (1976). *Annu. Rev. Biochem.* **45**, 861–888.
Morrison, R. T. & Boyd, R. N. (1973). *Organic Chemistry*, 3rd ed., pp. 787–802. Boston: Allyn & Bacon.
Otwinowski, Z. & Minor, W. (1995). *DENZO*. Yale University, New Haven, Connecticut, USA.
Pangborn, W., Erman, M., Li, N., Burkhart, B. M., Pletnev, V. Z., Duax, W. L., Gutierrez, R., Peirano, A., Eyzaguirre, J., Thiel, D. J. & Ghosh, D. (1996). *Proteins Struct. Funct. Genet.* **24**, 523–524.
Sack, J. S. (1988). *J. Mol. Graph.* **6**, 224–225.
Sheldrick, G. M. (1997). *SHELX*97 *Manual.* University of Göttingen, Germany.
Sigler, P. B. (1970). *Biochemistry*, **9**, 3609–3617.
Streitwieser, A. & Heathcock, C. H. (1985). *Introduction to Organic Chemistry*, 3rd ed., pp. 649–667. New York: McMillan.
Taurog, A., Dorris, M. L. & Doerge, D. R. (1996). *Arch. Biochem. Biophys.* **330**, 24–32.
Terwilliger, T. C. & Eisenberg, D. (1983). *Acta Cryst.* A**39**, 813–817.
Weeks, C. M., DeTitta, G. T., Hauptman, H. A., Thuman, P. & Miller, R. (1994). *Acta Cryst.* A**50**, 210–220.
Yang, W., Hendrickson, W. A., Crouch, R. J. & Satow, Y. (1990). *Science*, **249**, 1398–1405.